

Interactions and low energy collisions between an alkali ion and an alkali atom of different nucleus[†]

Arpita Rakshit^a, Chedli Ghanmi^{b,c}, Hamid Berriche^{b,c} and Bimalendu Deb^{e,d}

^a Sidhu Kanhu Birsa Polytechnic, Keshiary, Paschim Medinipur 721133, India.

^b Laboratory of Interfaces and Advanced Materials, Physics department, Faculty of Science, University of Monastir, 5019 Monastir, Tunisia.

^c Physics Department, Faculty of Science, King Khalid University, P. O. Box 9004, Abha, Saudi Arabia.

^d Department of Materials Science, ^e Raman Center for Atomic, Molecular and Optical Sciences, Indian Association for the Cultivation of Science, Jadavpur, Kolkata 700032, India.

We study theoretically interaction potentials and low energy collisions between different alkali atoms and alkali ions. Specifically, we consider systems like $X + Y^+$, where $X(Y^+)$ is either $\text{Li}(\text{Cs}^+)$ or $\text{Cs}(\text{Li}^+)$, $\text{Na}(\text{Cs}^+)$ or $\text{Cs}(\text{Na}^+)$ and $\text{Li}(\text{Rb}^+)$ or $\text{Rb}(\text{Li}^+)$. We calculate the molecular potentials of the ground and first two excited states of these three systems using pseudopotential method and compare our results with those obtained by others. We calculate ground-state scattering wave functions and cross sections of these systems for a wide range of energies. We find that, in order to get convergent results for the total scattering cross sections for energies of the order 1 K, one needs to take into account at least 60 partial waves. In the low energy limit ($< 1\mu\text{K}$), elastic scattering cross sections exhibit Wigner law threshold behavior while in the high energy limit the cross sections go as $E^{-1/3}$. We discuss qualitatively the possibilities of forming cold molecular ion by photoassociative spectroscopy.

I. INTRODUCTION

With recent developments in hybrid traps [1–5], both atoms and ions can be confined simultaneously within a single trap, facilitating the laboratory investigations on ion-atoms collisions in hitherto unexplored low energy regimes. Ion-atom scattering at low energy is important for a number of physical systems, such as cold plasmas, planetary atmospheres, interstellar clouds, etc. Gaining insight into the ion-atom interactions and scattering at ultra-low energy down to Wigner threshold law regime is important to understand charge transport[6] at low temperature, quantum reaction dynamics, polaron physics[7–9], ion-atom bound states[10], ion-atom photoassociation[11], etc. Several theoretical as well as experimental studies[5, 12–22] of atom-ion cold collisions have been carried out in recent times. It is proposed that controlled ion-atom cold collision can be utilized for quantum information processes [23, 24].

Ions are usually trapped by magnetic or radio-frequency fields. The major hindrance to cool magnetically trapped ions below milliKelvin temperature stems from the trap-induced micro-motion of the ions, which seems to be indispensable for a magnetic ion trap. Therefore, it is difficult to achieve sub-microKelvin temperature for an ion-atom system in a magnetic hybrid trap. But, to explore fully quantum or Wigner threshold law regime for ion-atom collisions, it is essential to reduce the temperature of ion-atom hybrid systems below one micro-Kelvin. One way to overcome this difficulty is to devise new methods to trap and cool both ions and atoms in an optical trap. With recent experimental demonstration of an optical trap for ions[25], the prospect for experimental explorations of ultracold ion-atom collisions in Wigner threshold regime and quantum degenerate charged systems in near future appears to be promising.

In the contexts of ion-atom cold collisions of current interest, there are mainly four types of ion-atom systems:(1) an alkaline metal ion interacting with an alkali metal atom, (2) a rare earth ion (such as Yb) interacting with an alkali metal

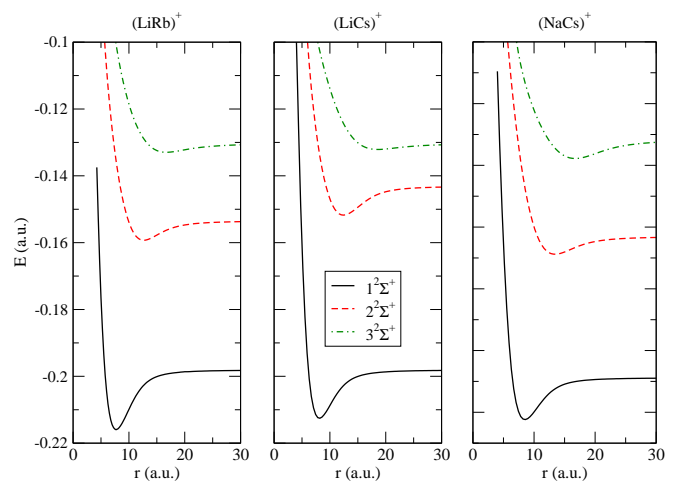


FIG. 1: (Color online) Adiabatic potential curves for $(\text{LiRb})^+$, $(\text{LiCs})^+$ and $(\text{NaCs})^+$

atom, (3) an alkali metal ion interacting with an alkali atom of the same nucleus and (4) an alkali metal ion interacting with an alkali atom of different nucleus. In the first two types, both the ion and the atom have one valence electron in the outermost shell. In the third type, the ion has closed shell structure while the atom has one valence electron in the outermost shell. Since both the ion and atom are of the same nucleus, there is center of symmetry for the electronic wave function of the ion-atom pair. Because of this symmetry, resonant charge transfer collision is possible in the third type. In the fourth type, the ion is of closed shell structure while the atom has one valence electron in the outermost shell. Since the nuclei of the atom and the ion are different, there is no resonant charge transfer collision in fourth type, though non-resonant charge transfer is possible in all the types. In the ultralow energy regime ($< \mu\text{K}$), non-resonant charge transfer collision is highly suppressed.

Here we study cold collision in the fourth type of ion-

atom systems. Our primary aim is to understand ground-state elastic scattering processes between an ion and an atom at ultralow energy where inelastic charge transfer process can be ignored. Due to the absence of resonance charge transfer reaction, the fourth type system is preferable for our purpose. A proper understanding of ground-state elastic scattering processes [19, 20] at low energy in an ion-atom system is important for exploring coherent control of ion-atom systems and formation of ultracold molecular ions by radiative processes[11].

Let a cold alkali metal ion A^+ interact with a cold alkali metal atom B . Suppose, the atomic mass of B is smaller than that of atom A . Then, for $(AB)^+$ molecular system, ground-state continuum asymptotically corresponds to the atom $B(ns)$ in 2S electronic state and the ion A^+ (complete shell) in 1S electronic state. In the separated atom limit, the first excited molecular potential asymptotically goes as the atom $A(ns)$ in 2S electronic state and alkali ion B^+ (complete shell) in 1S electronic state while the second electronic excited potential corresponds to $B(np)$ in 2P electronic state and alkali ion A^+ (complete shell) in 1S electronic state.

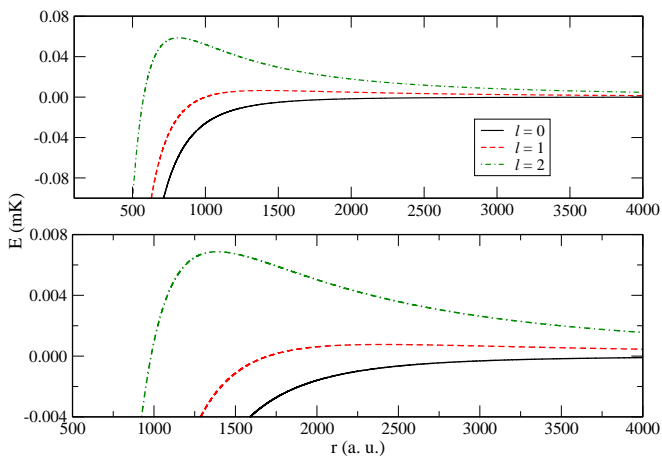


FIG. 2: (Color online) In the upper panel, the centrifugal energies for s (black, solid), p (red, dashed) and d (green, dashed-dotted) waves in mK are plotted against atom-ion separation for $1^2\Sigma^+$ state of $(LiCs)^+$ and the lower panel shows the same for $(NaCs)^+$.

We investigate cold collisions over a wide range of energies in three different alkali atom-alkali ion systems in the ground molecular potentials. The colliding atom-ion pairs we consider are: (i) $Cs^+ + Li$, (ii) $Cs^+ + Na$, and (iii) $Rb^+ + Li$. Since at ultralow energy, charge transfer reaction is highly suppressed in these systems, we study elastic scattering only. To calculate scattering wave functions, we need the data for Born-Oppenheimer adiabatic potentials of the systems. In the long range where the separation $r > 20a_0$ (a_0 is the Bohr radius), the potential is given by the sum of the dispersion terms, which in the leading order goes as $1/r^4$. We obtain short-range potentials by pseudopotential method. The short-range part is smoothly combined with the long-range part to obtain the potential for the entire range. We then solve time-independent Schroedinger equation for these potentials

with scattering boundary conditions by Numerov-Cooley algorithm. We present detailed results of scattering cross sections for these three systems over a wide range of energies.

II. INTERACTIONS AND MOLECULAR PROPERTIES

A. Adiabatic Potentials: Results and discussions

Under Born-Oppenheimer approximation, we compute the adiabatic potential energy curves of the $1^2\Sigma^+$, $2^2\Sigma^+$ and $3^2\Sigma^+$ electronic states of the three ionic molecules $(LiRb)^+$, $(LiCs)^+$ and $(NaCs)^+$ using the pseudopotential method proposed by Barthelat and Durand[26] in its semi-local form [27–30]. The interaction potentials between different alkali metal ion and an alkali metal atom were calculated by Valance[31] in 1978 by the method of pseudopotential.

The potential energy curves of the $1-3^2\Sigma^+$ electronic states, for the three ionic systems $(LiRb)^+$, $(LiCs)^+$ and $(NaCs)^+$, are calculated for a large and dense grid of internuclear distances ranging from 3 to 200 a.u. These states dissociate respectively, into $Li(2s \text{ and } 2p) + Rb^+$ and $Rb(5s) + Li^+$, $Li(2s \text{ and } 2p) + Cs^+$ and $Cs(6s) + Li^+$, and $Na(3s \text{ and } 3p) + Cs^+$ and $Cs(6s) + Na^+$. They are displayed in figure 1(a) for $LiRb^+$, 1(b) $LiCs^+$ and 1(c) for $NaCs^+$. For the three ionic systems, we remark, that the ground state has the deepest well compared to the $2^2\Sigma^+$ and $3^2\Sigma^+$ excited states. Their dissociation energies are of the order of several 1000 cm^{-1} . Their equilibrium positions lie at separations that are relatively larger than those of typical neutral alkali-alkali diatomic molecules.

The long range potential is given by the expression

$$V(r) = -\frac{1}{2} \left(\frac{C_4}{r^4} + \frac{C_6}{r^6} + \dots \right) \quad (1)$$

where C_4 , C_6 correspond to dipole, quadrupole polarisabilities of concerned atom. Hence, the long range interaction is predominately governed by polarisation interaction. Dipole polarisabilities for Na (3s) and Li (2s) are 162 a.u. and 164.14 a.u., respectively. One can define a characteristic length scale of the long-range potentials by $\beta = \sqrt{2\mu C_4/\hbar^2}$. The values of β for the collision of Li - Cs^+ pair and Na - Cs^+ pair are 1411.5 a.u. and 2405.8 a.u., respectively.

For ground state $1^2\Sigma^+$ potential, dissociation energy and equilibrium position are 2979 cm^{-1} and 8.51 a.u., respectively, for $(NaCs)^+$ while those for $(LiCs)^+$ are 3176 cm^{-1} and 8.12 a.u., respectively. Reduced mass for $(NaCs)^+$ and $(LiCs)^+$ are taken as 19.5995 a.u. and 6.6642 a.u., respectively.

B. Pseudopotential method

The use of the pseudopotential method, for each $(XY)^+$ ionic molecules $(LiRb^+, LiCs^+ \text{ and } NaCs^+)$, reduce the number of active electrons to only one electron. We have used a core polarization potential V_{CPP} for the simulation of the interaction between the polarizable X^+ and Y^+ cores with the

valence electron. This core polarization potential is used according to the formulation of Müller et al.[32], and is given by

$$V_{CPP} = -\frac{1}{2}\sum_{\lambda}\alpha_{\lambda}\vec{f}_{\lambda} \cdot \vec{f}_{\lambda} \quad (2)$$

where α_{λ} and \vec{f}_{λ} are respectively the dipole polarizability of the core λ , and the electric field produced by valence electrons and all other cores on the core λ . The electric field \vec{f}_{λ} is defined as:

$$\vec{f}_{\lambda} = \sum_i \frac{\vec{r}_{i\lambda}}{r_{i\lambda}^3} F(\vec{r}_{i\lambda}, \rho_{\lambda}) - \sum_{\lambda' \neq \lambda} \frac{\vec{R}_{\lambda',\lambda}}{R_{\lambda',\lambda}^3} Z_{\lambda} \quad (3)$$

where $\vec{r}_{i\lambda}$ and $\vec{R}_{\lambda',\lambda}$ are respectively the core-electron vector and the core-core vector.

Based on the formulation of Foucrault et al. [33] the cut-off function $F(\vec{r}_{i\lambda}, \rho_{\lambda})$ is a function of the quantum number l . In this formulation, the interactions of valence electrons of different spatial symmetry with core electrons are considered in a different way. The used cut-off radii of the lowest valence s , p , d and f one-electron for the Li, Na and Cs atoms are taken from ref.[27–30]. The extended Gaussian-type basis sets used for Li, Na, Rb and Cs atoms are respectively $(9s8p5d1f/8s6p3d1f)$ [29], $(7s6p5d3f/6s5p4d2f)$ [29], $(7s4p5d1f/6s4p4d1f)$ [34] and $(7s4p5d1f/6s4p4d1f)$ [28]. The used core polarizabilities of Li^+ , Na^+ , Rb^+ and Cs^+ cores are respectively $0.1915 a_0^3$, $0.993 a_0^3$, 9.245 and $15.117 a_0^3$ [32]. Using the pseudopotential technique each molecule is reduced to only one valence electron interacting with two cores. Within the Born-Oppenheimer approximation an SCF calculation, provide us with accurate potential energy curves and dipole functions.

C. Spectroscopic constants: Results and discussions

The spectroscopic constants ($R_e, D_e, T_e, \omega_e, \omega_e \chi_e, B_e$) of the $1-3^2\Sigma^+$ electronic states are presented in tables 1-3 for $(\text{LiRb})^+$, $(\text{LiCs})^+$ and $(\text{NaCs})^+$ respectively. Table 1 presents the spectroscopic constants of $(\text{LiRb})^+$ compared with the other theoretical works[35–38]. To the best of our knowledge, the only theoretical works performed for $(\text{LiRb})^+$ molecular ion are those of Patil et al.[37] and Azizi et al.[38] and no experimental spectroscopic information have been found on such system. Azizi et al.[38] reported the spectroscopic constants for many ionic alkali dimers but only for the ground and the first excited states. They have used in their study a similar formalism as used in our work. As it seems from table 1, there is a good agreement between the available theoretical works[35–38] and our ab initio study. In addition, our ground state equilibrium distance (R_e) presents a satisfying agreement as well as the well depth (D_e) with the work of Azizi et al.[38]. We found for (R_e) and (D_e), respectively, 7.70 a. u. and 3912 cm^{-1} and they found 7.54 a. u. and 4193 cm^{-1} . The same agreement is observed between our harmonicity frequency (ω_e) and that of Azizi et al.[38]. The difference between the two values is 2.09 cm^{-1} . There is also

a very good agreement between our equilibrium distance and that of Patil et al.[37] ($R_e = 7.60$ a. u.), in contrast to their well depth[37], which is underestimated ($D_e = 3432 \text{ cm}^{-1}$). For the first excited state, Azizi et al.[38] reported the spectroscopic constants $R_e = 12.60$ a. u., $D_e = 1306 \text{ cm}^{-1}$ and $\omega_e = 63.00 \text{ cm}^{-1}$ to be compared with our values of, respectively, 12.67 a. u., 1270 and 63.73 cm^{-1} .

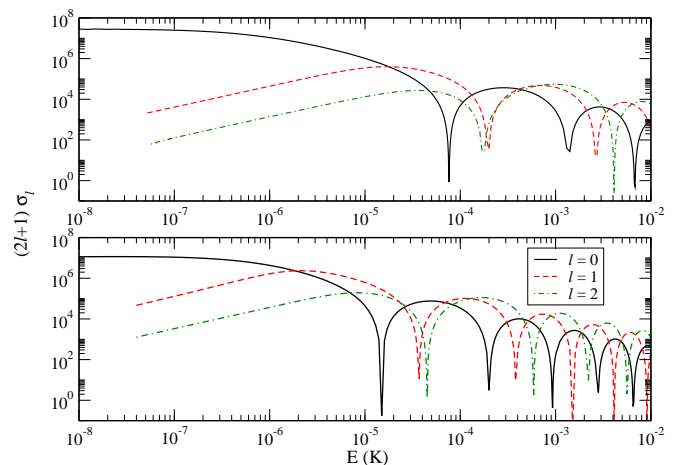


FIG. 3: (Color online) s - p - and d -wave scattering cross sections are plotted against E in K for $1^2\Sigma^+$ state of $(\text{LiCs})^+$ and $(\text{NaCs})^+$ in upper and lower panel, respectively.

The spectroscopic constants of $(\text{LiCs})^+$ and $(\text{NaCs})^+$, are present respectively in tables 2 and 3 and compared with the available theoretical results[31, 39]. To the best of our knowledge there is no experimental data for these ionic molecules. For the $(\text{LiCs})^+$ ionic molecule, we compare our results only with the theoretical work of Khelifi et al.[39] where they have used a similar method as used in our work. They reported for the ground state $1^2\Sigma^+$ the spectroscopic constant $R_e = 7.91$ a. u. and $D_e = 3543 \text{ cm}^{-1}$ to be compared with our values of, respectively, $R_e = 8.12$ a. u. and $D_e = 3176 \text{ cm}^{-1}$. A rather good agreement is observed for the equilibrium distance, however, their potential is much deeper. The same good agreement between our spectroscopic constant and those of Khelifi et al.[39] is observed for the $2^2\Sigma^+$ and $3^2\Sigma^+$ states. For the ground state of $(\text{NaCs})^+$ ionic molecule, there are a good agreement between our well depth, as well as the equilibrium distance with the theoretical results of Valence[31]. We found a well depth of 2979 cm^{-1} located at 8.51 a. u., while valence[31] found, respectively, 3388 cm^{-1} located at 7.60 a. u.. In contrast to the ground state, where the agreement between our work and those of Valence[31] is good, there is a disagreement for the $2^2\Sigma^+$ and $3^2\Sigma^+$ states. The two states exhibit small potential wells in the Valence's work equal respectively, 774 and 732 cm^{-1} , while they present in our work a significant well depth of, respectively, 1262 and 1393 cm^{-1} .

TABLE I: A comparison of the spectroscopic constants for the ground ($X^2\Sigma^+$) and the first and second excited ($2^2\Sigma^+$ and $3^2\Sigma^+$) electronic states of $(\text{LiRb})^+$ molecular ion with the available works[35–38]

state	R_e (a.u.)	D_e (cm^{-1})	T_e (cm^{-1})	ω_e (cm^{-1})	$\omega_e\chi_e$ (cm^{-1})	B_e (cm^{-1})	references
$X^2\Sigma^+$	7.70	3912		137.56	1.67	0.158098	This work
		3705					[35]
	7.50						[36]
	7.60	3432					[37]
$2^2\Sigma^+$	7.54	4193		139.65			[38]
	12.67	1270	12438	63.73	0.51	0.058456	this work
$3^2\Sigma^+$	12.60	1306		63.00			[38]
	16.66	617	18200	35.73	1.55	0.033769	This work

TABLE II: A comparison of the spectroscopic constants for the ground ($X^2\Sigma^+$) and the first and second excited ($2^2\Sigma^+$ and $3^2\Sigma^+$) electronic states of $(\text{LiCs})^+$ molecular ion with the work Khelifi et al.[39]

state	R_e (a.u.)	D_e (cm^{-1})	T_e (cm^{-1})	ω_e (cm^{-1})	$\omega_e\chi_e$ (cm^{-1})	B_e (cm^{-1})	references
$1^2\Sigma^+$	8.12	3176	0	124.46	1.08	0.138337	This work
	7.19	3543					[39]
$2^2\Sigma^+$	12.42	1911	13343	68.69	0.63	0.059126	This work
	12.37	2022	19553				[39]
$3^2\Sigma^+$	18.53	422	17660	28.07	1.29	0.026570	This work

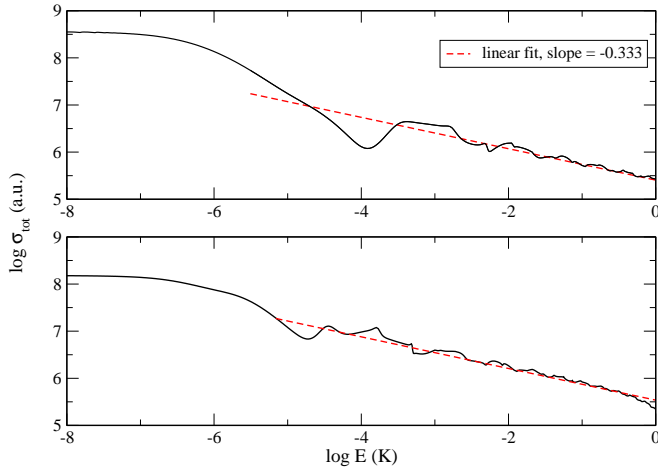


FIG. 4: (Color online) Total scattering cross sections in a.u.as a function of energy in K for electronic ground-state $1^2\Sigma^+$ of $(\text{LiCs})^+$ and $(\text{NaCs})^+$ are plotted in upper and lower panel, respectively.

III. ELASTIC COLLISIONS: RESULTS AND DISCUSSIONS

Here we present results on elastic collisions of the discussed ion-atom systems making use of the interaction potentials calculated above. In particular we focus on low energy collisions. Using the well-known expansion of continuum state in terms of partial waves, the wave function $\psi_\ell(kr)$ for ℓ th partial wave is given by

$$\left[\frac{d^2}{dr^2} + k^2 - \frac{2\mu}{\hbar^2}V(r) - \frac{\ell(\ell+1)}{r^2} \right] \psi_\ell(kr) = 0 \quad (4)$$

subject to the standard scattering boundary condition $\psi_\ell(kr) \sim \sin[kr - \ell\pi/2 + \eta_\ell]$. Here r denotes the ion-atom separation, the wave number k is related to the collision energy E by $E = \hbar^2 k^2 / 2\mu$ and μ stands for the reduced mass of the ion-atom pair. The total elastic scattering cross section is given by

$$\sigma_{el} = \frac{4\pi}{k^2} \sum_{\ell=0}^{\infty} (2\ell+1) \sin^2(\eta_\ell) \quad (5)$$

To know the relevant energy regimes where s - p - and d -wave collisions are important, we have plotted in figure 2 the centrifugal energies for first 3 partial waves ($\ell = 0, 1$ and 2) against ion-atom separations for ground state $1^2\Sigma^+$ of $(\text{NaCs})^+$ and $(\text{LiCs})^+$, respectively. For d -wave, the values of centrifugal barrier are about 0.007 mK for $(\text{NaCs})^+$ and about 0.06 mK for $(\text{LiCs})^+$. These values indicate that the potential energy barriers for low lying higher partial waves are very low for atom-ion systems allowing tunneling of the wave function towards the inner region of the barriers. Unlike atom-atom systems at low energy, a number of partial waves can significantly contribute to the ion-atom scattering cross section at low energy.

In figure 3, the partial-wave cross sections for ground $1^2\Sigma^+$ state collisions are plotted against collision energy E in K for $(\text{NaCs})^+$ and $(\text{LiCs})^+$. As $k \rightarrow 0$, s -wave cross section becomes independent of energy while p - and d -wave cross sections vary in accordance with Wigner threshold laws. According to Wigner threshold laws, as $k \rightarrow 0$, the phase shift for ℓ th partial-wave $\eta_\ell \sim k^{2\ell+1}$ if $\ell \leq (n-3)/2$, otherwise $\eta_\ell \sim k^{n-2}$ for a long range potential behaving as $1/r^n$. Since Born-Oppenheimer ion-atom potential goes as $1/r^4$ in the asymptotic limit, as $k \rightarrow 0$, s -wave scattering cross section becomes independent of energy (or k) while all other higher partial-wave cross sections go as $\sim k^2$. In the Wigner

TABLE III: A comparison of the spectroscopic constants for the ground ($X^2\Sigma^+$) and the first and second excited ($2^2\Sigma^+$ and $3^2\Sigma^+$) electronic states of $(\text{NaCs})^+$ molecular ion with the work of Valence[31]

state	R_e (a.u.)	D_e (cm^{-1})	T_e (cm^{-1})	ω_e (cm^{-1})	$\omega_e\chi_e$ (cm^{-1})	B_e (cm^{-1})	references
$1^2\Sigma^+$	8.51	2979	0	68.17	0.32	0.042418	This work
	7.60	3388					[31]
$2^2\Sigma^+$	13.45	1262	11758	33.98	0.30	0.016977	This work
	14.20	774					[31]
$3^2\Sigma^+$	16.77	1393	18553	26.20	1.69	0.010920	This work
	15.00	732					[31]

threshold regime, hetero-nuclear ion-atom collisions are dominated by elastic scattering processes since the charge transfer reactions are highly suppressed in this energy regime. Fur-

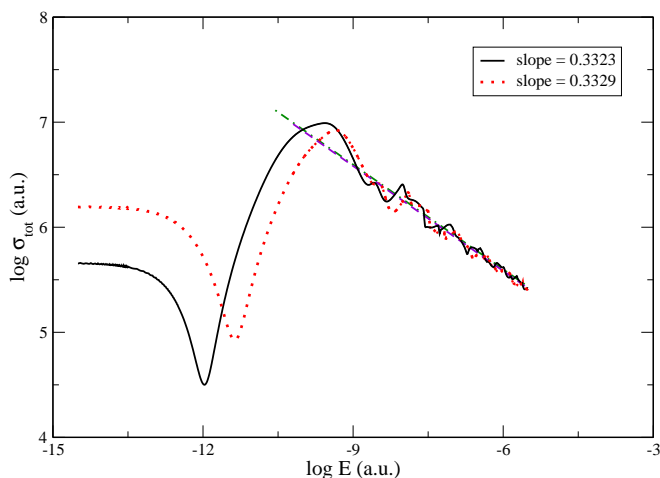


FIG. 5: (Color online) Total elastic scattering cross-section σ_{tot} for $\text{Li} + {}^{87}\text{Rb}^+$ ($1^2\Sigma^+$) collision is plotted against collision energy E in K where the black solid line and red dotted line are for ${}^7\text{Li}$ and ${}^6\text{Li}$, respectively. Blue dashed and green dashed-dotted lines are the corresponding linear fits for energies greater than 10^{-6} K. Both cases follow one-third law and the intercepts are 3.587 and 3.606 in a.u. for ${}^6\text{Li}$ and ${}^7\text{Li}$, respectively where as the theoretically calculated values are 3.3269 and 3.3476 in a.u., respectively.

In figure 4, we have plotted logarithm of total elastic scattering cross sections (σ_{tot}) expressed in a.u. as a function of logarithm of E in K for ground state collisions between Li and Cs^+ and between Na and Cs^+ , respectively. For both $(\text{LiCs})^+$ and $(\text{NaCs})^+$, to calculate σ_{tot} , we require more than 60 partial waves to get converging results for energies greater than 1 mK. In the large energy limit, the cross section behaves as

$$\sigma_{tot} \sim \pi \left(\frac{\mu C_4^2}{\hbar^2} \right)^{\frac{1}{3}} \left(1 + \frac{\pi^2}{16} \right) E^{-\frac{1}{3}} \quad (6)$$

Thus, in the large energy regime the slope of the logarithm of σ_{tot} as a function of $\log E$ is a straight line obeying the equation $\sigma_{tot}(E) = -(1/3)E + c_E$ where the slope of the line is $-1/3$ and the intercept of the line on the energy axis is solely determined by the C_4 coefficient of long-range part of

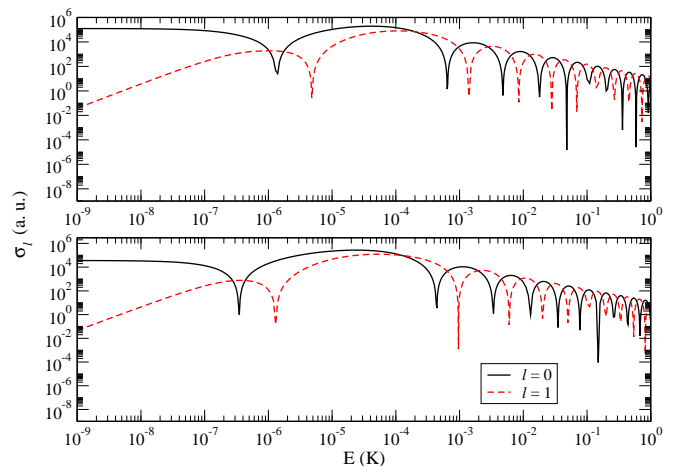


FIG. 6: (Color online) Partial wave cross sections for ${}^6\text{Li} + \text{Rb}^+$ ($1^2\Sigma^+$) and ${}^7\text{Li} + \text{Rb}^+$ ($1^2\Sigma^+$) collision are plotted as a function of E (in K) for $\ell = 0$ (solid) and $\ell = 1$ (dashed) in upper and lower panel, respectively.

the potential, or equivalently by the characteristic length scale β of the potentials or the polarisability of the neutral atom interacting with the ion. As shown in figure 4, we have numerically verified this $E^{-1/3}$ law for both $\text{Li}-\text{Cs}^+$ and $\text{Na}-\text{Cs}^+$ systems. The linear fit to the plot of numerically calculated σ_{tot} against in the large energy regime shows that the value of the slope is quite close to the actual value of $1/3$. Since the dipole polarizability of Li and Na is not much different, one can expect that for both $\text{Li}-\text{Cs}^+$ and $\text{Na}-\text{Cs}^+$ systems, the energy-dependence of σ_{tot} at large energy should be similar. In fact, figure 4 shows that for energies much greater $1 \mu\text{K}$, both systems exhibit similar asymptotic energy dependence.

Finally, we consider the collision of ${}^{85}\text{Rb}^+$ with the two isotopes of Li atom, namely, ${}^6\text{Li}$ and ${}^7\text{Li}$, and the results are shown in figures 5 and 6. The purpose here is to investigate the isotopic effects of Li on low energy collisions with ${}^{85}\text{Rb}^+$ ion. In figure 5 we have plotted logarithm (to the base of 10) of σ_{tot} as a function of logarithm (to the base of 10) of E . Results clearly show that the patterns are same for ${}^6\text{Li}$ and ${}^7\text{Li}$ colliding with ${}^{85}\text{Rb}^+$, but they differ in magnitudes, particularly in the low energy regime. Figure 6 exhibits the variation of s - and p -wave scattering cross sections against energy in log-log scale for both isotopes of Li colliding with Rb^+ . Again, the results are qualitatively similar for both the isotopes, but they differ slightly quantitatively. Comparing

the upper and lower panels in figure 6, one can notice that the Wigner threshold law regime for ${}^6\text{Li}$ can be attained at slightly higher energy than that for ${}^7\text{Li}$. This can be understood quite easily in the following way. The ultralow energy collisional properties are primarily determined by the nature of the long-range potentials. Since the long-range parts of both ${}^6\text{Li-Rb}^+$ and ${}^7\text{Li-Rb}^+$ potentials are same, the difference in ultralow energy collision cross sections at a fixed collision energy $\hbar^2 k^2 / (2\mu)$ can only arise due to the difference in wave numbers. Since for a fixed collision energy, the value of k for ${}^6\text{Li-Rb}^+$ system is smaller than that for ${}^7\text{Li-Rb}^+$ system, the zero energy limit ($k \rightarrow 0$) for ${}^6\text{Li-Rb}^+$ system is expected to reach at a slightly higher collision energy compared to ${}^7\text{Li-Rb}^+$ system.

IV. CONCLUSIONS

In conclusions, we have calculated ion-atom interaction potentials, molecular spectroscopic constants and low energy elastic cross sections for 3 ion-atom systems, namely, $\text{Li} + \text{Cs}^+$, $\text{Na} + \text{Cs}^+$, and $\text{Li} + \text{Rb}^+$. We have compared and analysed the results for these 3 systems. The reasons for choosing these 3 particular systems for our study are two-fold. First,

all of them have almost same long-range coefficient C_4 or the characteristic length scale β that characterises the low energy ion-atom collisional properties. Second, they are of different nuclei, allowing us to ignore charge transfer reactions at ultralow energy. The low energy scattering results presented here may be useful for future exploration for photoassociative formation of cold diatomic molecular ions from these 3 ion-atom systems. The colliding ground state atom-ion pair corresponding to the continuum of $1^2\Sigma^+$ may be photoassociated to form a bound state in second excited potential $3^2\Sigma^+$ by using a laser of appropriate frequency. This is promising because the transition is dipole allowed and is similar to atomic transition. The formation of such cold molecular ions by radiative processes will pave new directions to ultracold chemistry.

Acknowledgments

This work is jointly supported by Department of Science and Technology (DST), Ministry of Science and Technology, Government of India and Ministry of Higher Education and Scientific Research (MHESR), Government of Tunisia, under an India-Tunisia project for bilateral scientific cooperation.

-
- [1] W. W. Smith, O. P. Marakov, and J. Lin, *J. of Mod. Opts.* **52**, 2253 (2005).
- [2] C. Zipkes, S. Palzer, C. Sias, and M. Kohl, *Nat. Lett.* **464**, 388 (2010).
- [3] C. Zipkes, S. Palzer, L. Ratschbacher, C. Sias, and M. Kohl, *Phys. Rev. Lett.* **105**, 133201 (2010).
- [4] A. T. Grier, M. Certina, F. Orucevic, and V. Vuletic, *Phys. Rev. Lett.* **102**, 223201 (2009).
- [5] D. S. Goodman, J. E. Wells, J. M. Kwolek, R. Blumel, F. A. Narducci, and W. W. Smith, *Phys. Rev. A* **91**, 012709 (2015).
- [6] R. Côté, *Phys. Rev. Lett.* **85**, 5316 (2000).
- [7] P. Massignan, C. J. Pethick, and H. Smith, *Phys. Rev. A* **71**, 023606 (2005).
- [8] R. M. Kalas and D. Blume, *Phys. Rev. A* **73**, 043608 (2006).
- [9] F. M. Cucchiatti and E. Timmermans, *Phys. Rev. Lett.* **96**, 210401 (2006).
- [10] R. Côté, V. Kharchenko, and M. D. Lukin, *Phys. Rev. Lett.* **89**, 093001 (2002).
- [11] A. Rakshit and B. Deb, *Phys. Rev. A* **83**, 022703 (2011).
- [12] S. Schmid, A. Härter, and J. H. Denschlag, *Phys. Rev. Lett.* **105**, 133202 (2010).
- [13] E. Bodo, P. Zhang, and A. Dalgarno, *New J. Phys.* **10**, 033024 (2008).
- [14] P. Zhang, E. Bodo, and A. Dalgarno, *J. Phys. Chem. A* **113**, 15085 (2009).
- [15] R. Côté and A. Dalgarno, *Phys. Rev. A* **62**, 012709 (2000).
- [16] B. Zygelman, A. Dalgarno, M. Kimura, and N. F. Lane, *Phys. Rev. A* **40**, 2340 (1989).
- [17] P. Zhang, E. Bodo, and A. Dalgarno, *J. Phys. Chem.* **133**, 15085 (2009).
- [18] Z. Idziaszek, T. Calarco, P. S. Julienne, and A. Simoni, *Phys. Rev. A* **79**, 010702(R) (2009).
- [19] B. Gao, *Phys. Rev. Lett.* **104**, 213201 (2010).
- [20] M. Li and B. Gao, *Phys. Rev. A* **86**, 012707 (2012).
- [21] E. R. Sayfutyarova, A. A. Buchachenko, S. A. Yakovleva, and A. K. Belyaev, *Phys. Rev. A* **87**, 052717 (2013).
- [22] F. H. J. Hall, P. Eberle, G. Hegi, M. Raoult, M. Aymar, O. Dulieu, and S. Willitsch, *Mol. Phys.* **111**, 2020 (2013).
- [23] H. Doerk, Z. Idziaszek, and T. Calarco, *Phys. Rev. A* **81**, 012708 (2010).
- [24] A. Harter and J. H. Denschlag, *Contemporary Phys.* **55**, 33 (2014).
- [25] T. Huber, A. Lambrecht, J. Schmidt, L. Karpa, and T. Schaetz, *Nature* **5**, 5587 (2014).
- [26] J. C. Barthelat and P. Durand, *Theor. Chem. Acta.* **38**, 283 (1975).
- [27] C. Ghanmi, H. Berriche, and H. B. Ouada, *J. Mol. Spectr.* **235**, 158 (2006).
- [28] C. Ghanmi, M. Farjallah, and H. Berriche, *Int. J. Quant. Chem.* **112**, 2403 (2012).
- [29] H. Berriche, *J. Mol. Struct. (Theochem)* **663**, 101 (2003).
- [30] H. Berriche, C. Ghanmi, and H. B. Ouada, *J. Mol. Spectr.* **230**, 161 (2005).
- [31] A. Valence, *J. Chem. Phys.* **69**, 355 (1978).
- [32] W. Muller, J. Flesh, and W. Meyer, *J. Chem. Phys.* **80**, 3297 (1984).
- [33] M. Foucrault, P. Millie, and J. P. Daudey, *J. Chem. Phys.* **96**, 1257 (1992).
- [34] D. Pavolini, T. Gustavsson, F. Spiegelmann, and J. P. Daudey, *J. Phys. B At. Mol. Opt. Phys.* **22**, 1721 (1989).
- [35] L. Bellomonte, P. Cavaliere, and G. Ferrante, *J. Chem. Phys.* **61**, 3225 (1974).
- [36] S. H. Patil and K. T. Tang, *Phys. Rev. Lett.* **45**, 18 (1980).
- [37] S. H. Patil and K. T. Tang, *P. Cem. Phys.* **113**, 676 (2000).
- [38] S. Azizi, M. Aymar, and O. Dulieu, *AIP. Conf. Proc.* **935**, 164 (2007).

- [39] N. Khelifi, R. Dardouri, and O. M. Al-Dossary, *J. Appl. Spect.* **78**, 11 (2011).

